

Molybdenum Adsorption on Oxides, Clay Minerals, and Soils

Sabine Goldberg,* H. S. Forster, and C. L. Godfrey

ABSTRACT

Molybdenum adsorption behavior was investigated on various crystalline and x-ray amorphous Al and Fe oxide minerals, clay minerals, CaCO₃, and arid-zone calcareous and noncalcareous soils. Molybdenum adsorption on both Al and Fe oxides exhibited a maximum at low pH extending to about pH 4 to 5. Above pH 5 adsorption decreased rapidly, with little adsorption occurring above pH 8. Molybdenum adsorption was higher for the oxide minerals having higher specific surface area and lower crystallinity. Molybdenum adsorption on the clay minerals exhibited a peak near pH 3 and then decreased rapidly with increasing pH until adsorption was virtually zero near pH 7. The magnitude of Mo adsorption on clays increased in the order: kaolinite < illite < montmorillonite. Shifts in point of zero charge were observed on Al and Fe oxides and kaolinite following Mo adsorption, indicating an inner-sphere adsorption mechanism for Mo on these surfaces. Molybdenum adsorption behavior on three arid-zone noncalcareous soils resembled that on clays, exhibiting a peak near pH 3 to 4 and decreasing with increasing pH up to pH 7. This behavior is expected since the oxide content of these soils is low. Molybdenum adsorption on calcite and two calcareous arid-zone soils was low, indicating that CaCO₃ is not a significant sink for Mo in soils.

MOLYBDENUM IS A TRACE ELEMENT required by both plants and animals. Molybdenum is readily taken up by plants and can accumulate to levels detrimental to grazing ruminants (Reisenauer et al., 1962). Especially in contrast to phosphate, studies of Mo adsorption are limited.

Molybdenum adsorption by Al and Fe oxides has been investigated (Jones, 1957; Reisenauer et al., 1962; Reyes and Jurinak, 1967; Kyriacou, 1967; McKenzie, 1983; Ferreiro et al., 1985; Zhang and Sparks, 1989; Vordonis et al., 1990; Spanos et al., 1990a,b; Bibak and Borggaard, 1994). Molybdenum adsorption was studied on halloysite, nontronite, and kaolinite (Jones, 1957), kaolinite, montmorillonite, and illite (Motta and Miranda, 1989), and kaolinite (Phelan and Mattigod, 1984; Mikkonen and Tummavuori, 1993). Molybdenum adsorption by soils has been investigated previously (Jones, 1957; Reisenauer et al., 1962; Barrow, 1970; Theng, 1971; Gonzalez et al., 1974; Jarrell and Dawson, 1978; Karimian and Cox, 1978; Roy et al., 1986, 1989; Xie and MacKenzie, 1991; Xie et al., 1993; Mikkonen and Tummavuori, 1993).

Iron oxide adsorbed more Mo than did Al oxide (Jones, 1957). Molybdenum adsorption on oxides increased from pH 2 to 4, exhibited a peak near pH 4, and decreased with increasing pH above 4 (Jones, 1957; Kyriacou,

1967; McKenzie, 1983; Ferreiro et al., 1985). The decrease in adsorption with increasing pH above 4 occurred more rapidly for Al oxide than for Fe oxide (Ferreiro et al., 1985).

The mechanism of Mo adsorption on Al and Fe oxides is suggested to be ligand exchange with surface hydroxyl ions (Jones, 1957; Ferreiro et al., 1985). Ligand exchange is a mechanism by which ions become specifically adsorbed as inner-sphere surface complexes. Inner-sphere surface complexes contain no water molecules between the adsorbing ion and the surface functional group (Spósito, 1984). The point of zero charge (PZC) of variable-charge minerals is shifted to a more acid pH value following specific adsorption of anions. Molybdenum adsorption lowered the PZC of goethite, indicating specific adsorption (McKenzie, 1983). By studying the effects of ionic strength on anion adsorption, Hayes et al. (1988) were able to distinguish between inner- and outer-sphere Se surface complexes. Outer-sphere surface complexes contain at least one water molecule between the adsorbing ion and the surface functional group (Spósito, 1984). Hayes et al. (1988) suggested that since selenite showed little ionic strength dependence in its adsorption behavior, it was specifically adsorbed on goethite in an inner-sphere surface complex. Zhang and Sparks (1989) found little ionic strength dependence for Mo adsorption on goethite and interpreted this result as supporting evidence for inner-sphere surface complexation.

Molybdenum adsorption on the clay minerals metahalloysite, nontronite, and kaolinite showed pH-dependent adsorption behavior similar to that on oxides with an adsorption peak near pH 4 (Jones, 1957; Mikkonen and Tummavuori, 1993). The relative adsorption on the clay minerals was less than on Al and Fe oxide and decreased in the order: metahalloysite > nontronite > kaolinite (Jones, 1957) and montmorillonite > kaolinite > illite (Motta and Miranda, 1989). Similar behavior was observed for a soil clay dominant in kaolinite and illite (Theng, 1971). Adsorption on soil clays was decreased by removal of amorphous Fe and Al oxides (Theng, 1971).

Molybdenum adsorption by soils has been investigated (Jones, 1957; Reisenauer et al., 1962; Barrow, 1970; Roy et al., 1986, 1989). Adsorption of Mo was highly correlated with extractable Al (Barrow, 1970) and Fe (Gonzalez et al., 1974; Jarrell and Dawson, 1978; Karimian and Cox, 1978). Removal of amorphous Fe oxides drastically reduced Mo adsorption by an Australian soil (Jones, 1957). The pH dependence of Mo adsorption on soil resembled that on oxides and clay minerals. Adsorption increased with increasing pH up to a peak near pH 4 and then decreased with increasing pH above

USDA-ARS, U.S. Salinity Lab., 450 Big Springs Rd., Riverside, CA 92507. Contribution from the U.S. Salinity Lab. Received 18 Jan. 1995.
 *Corresponding author.

Table 1. Characterization of oxides and clay minerals used in this study.

Solid	Surface area	Point of zero charge	Trace impurities
	$\text{m}^2 \text{g}^{-1}$		
hematite	10.9		none
goethite	63.1	8.82	none
poorly crystalline goethite	148.8	7.83	none
amorphous Fe oxide	222.7	7.23	
Aluminum Oxid C	102.9	9.30	none
gibbsite	56.5	9.41	none
amorphous Al oxide	209.9	9.30	
calcite	22.0		none
KGa-1 kaolinite	9.14	2.88	vermiculite, feldspar
KGa-2 kaolinite	19.3	2.93	chlorite
SWy-1 montmorillonite	18.6		mica
SAz-1 montmorillonite	48.9		none
STx-1 montmorillonite	70.3		none
IMt-1 illite	24.9		kaolinite, vermiculite

4 (Jones, 1957; Gonzalez et al., 1974; Mikkonen and Tummavuori, 1993).

The constant capacitance model is a chemical surface complexation model that uses a ligand exchange mechanism to describe specific anion adsorption (Stumm et al., 1980). The model explicitly defines inner-sphere surface complexes and chemical reactions and considers the charge on both the adsorbate anion and the adsorbent surface. The constant capacitance model has been used successfully to describe phosphate (Goldberg and Spósito, 1984a) and borate (Goldberg and Glaubig, 1985) adsorption on various Al and Fe oxides via ligand exchange with surface hydroxyls, borate adsorption on clay minerals via ligand exchange with aluminum groups (Goldberg and Glaubig, 1986a), and phosphate (Goldberg and Spósito, 1984b) and borate adsorption (Goldberg and Glaubig, 1986b) on soils as a function of solution pH. The constant capacitance model has successfully described molybdate adsorption on the clay minerals kaolinite, montmorillonite, and illite as a function of equilibrium Mo concentration (Motta and Miranda, 1989).

This study was initiated to evaluate the Mo adsorption behavior of a variety of soils and soil minerals: Al oxide, Fe oxide, calcite, and clay minerals. Molybdenum adsorption as a function of pH on these materials was evaluated and compared. The ability of the constant capacitance model to describe molybdate adsorption on these surfaces was also investigated.

MATERIALS AND METHODS

Molybdenum adsorption behavior was studied on various adsorbents. Hematite was obtained from Fisher Scientific Co. (Fair Lawn, NJ) and Aluminium Oxid C ($\delta\text{-Al}_2\text{O}_3$) from Degussa (Teterboro, NJ). Goethite, $\alpha\text{-FeOOH}$, poorly crystalline goethite, and amorphous Al oxide were synthesized as described by McLaughlin et al. (1981). Gibbsite, $\alpha\text{-Al(OH)}_3$, was synthesized according to the procedure of Kyle et al. (1975) and amorphous Fe oxide was synthesized as described by Sims and Bingham (1968). The oxide mineralogy was verified using x-ray diffraction analysis. The calcite was Multifex obtained from Pfizer (New York, NY). Samples of kaolinite (KGa-1 and KGa-2), montmorillonite (SWy-1, SAz-1, and STx-1), and illite (IMt-1) were obtained from the Clay Minerals Society's Source Clays Repository (Univ. of Missouri, Columbia). The kaolinites and montmorillonites were used without pretreatment. The illite was ground to pass a 0.05mm sieve. Surface samples of the Imperial, Twisselman, Pachappa, Porterville, and Hesperia soil series consisted of the <2-mm fraction. Organic and inorganic C analyses were conducted as described by Nelson and Sommers (1982). Free Al and Fe oxides were extracted using the method of Coffin (1963).

Trace impurities in the clay minerals and oxides were determined using x-ray diffraction powder mounts (see Table 1). To obtain dominant clay minerals in the soils, x-ray diffraction peak areas obtained using oriented mounts were converted directly to clay mineral contents using the method of Klages and Hopper (1982). Specific surface areas of the clay minerals, oxides, and calcite were determined with a single-point BET N_2 adsorption isotherm obtained using a Quantasorb Jr. surface area analyzer (Quantachrome Corp., Syosset, NY). Specific surface areas of the soil samples were obtained using ethylene glycol monoether adsorption as described by Cihacek and Bremner (1979). Table 1 presents mineralogical, point of zero charge, and specific surface area data for the oxides and clay minerals. Table 2 presents classifications, chemical and mineralogical data, and specific surface area values for the soils.

Points of zero charge and electrophoretic mobilities were determined for all oxides and kaolinites by microelectrophoresis using a Zeta-Meter 3.0 system (Zeta Meter, Long Island City, NY). The electrophoretic mobilities of suspensions containing 0.01% solid in 0.01 M NaCl were determined at various pH values. The PZCs were obtained by interpolation of the data to zero electrophoretic mobility. Electrophoretic mobility measurements were also determined in the presence of 0.0104, 0.0521, and 0.292 mol Mo m^{-3} .

Molybdenum adsorption experiments were carried out in batch systems to determine adsorption envelopes (amount of

Table 2. Characterization of soils used in this study.

Soil	Inorganic C	Organic C	Free Al	Free Fe	Surface area	Dominant minerals
Imperial fine, montmorillonitic (calcareous), Vertic Torrifluent	1.88	0.89	0.038	0.61	196.0	kaolinite, montmorillonite, illite
Twisselman fine, mixed (calcareous), thermic Typic Torriorthent	0.170	0.56	0.063	0.30	182.4	kaolinite, montmorillonite, illite
Pachappa coarse-loamy, mixed, thermic Mollic Haploxeralf	0.010	0.49	0.067	0.76	36.3	illite, kaolinite, montmorillonite
Porterville fine, montmorillonitic, thermic Typic Chromoxerert	0.023	0.84	0.090	1.07	172.2	kaolinite, illite, montmorillonite
Hesperia coarse-loamv. mixed. nonacid. thermic Xeric Torriorthent	0.001	0.44	0.034	0.32	30.9	illite, kaolinite, montmorillonite

Table 3. Suspension densities and intrinsic surface complexation constants for the oxides and clay minerals used in this study.

Solid	Suspension density g L ⁻¹	Log K ₊ (int)	Log K ₋ (int)	Log K _{Mo} (int)	Log K _{Mo} (int)
hematite	5.0	7.31	- 8.80	10.53	5.64
goethite	1.25	7.31	- 8.80	9.15	- †
poorly crystalline goethite	0.64	7.31	- 8.80	10.36	4.31
amorphous Fe oxide	0.64	7.31	- 8.80	9.95	
Aluminium Oxid C	4.0	1.38	- 9.09	11.37	
gibbsite	1.25	7.38	- 9.09	10.03	3.82
amorphous Al oxide	0.35	7.38	- 9.09	9.41	2.36
KGa-1 kaolinite	200	4.82	- 6.25	7.83	
KGa-2 kaolinite	100	4.32	- 9.09	1.14	1.53
SWy-1 montmorillonite	30	2.75	- 9.09	5.75	
SAz-1 montmorillonite	40	2.43	-2.69	1.32	
STx-1 montmorillonite	40	2.96	-9.09	5.67	
IMt-1 illite	50	7.38	0.05	11.03	

† No convergence.

Mo adsorbed as a function of solution pH per fixed total Mo concentration). Samples of adsorbent were added to 50-mL polypropylene centrifuge tubes and equilibrated with aliquots (see Table 3 for suspension densities) of a 0.1 M NaCl solution by shaking for 20 h on a reciprocating shaker at 23 ± 0.5°C. This solution contained 0.292 or 1.04 mol Mo m⁻³ from Na₂MoO₄·2H₂O (Mallinckrodt, St. Louis, MO) and had been

adjusted to the desired pH values using 1 M HCl or 1 M NaOH additions that changed the total volume by ≤ 2%. The samples were centrifuged at a relative centrifugal force of 7800 X g for 20 min. The decantates were analyzed for pH, filtered through a 0.45-μm Whatman filter, and analyzed for Mo concentration using inductively coupled plasma emission spectrometry.

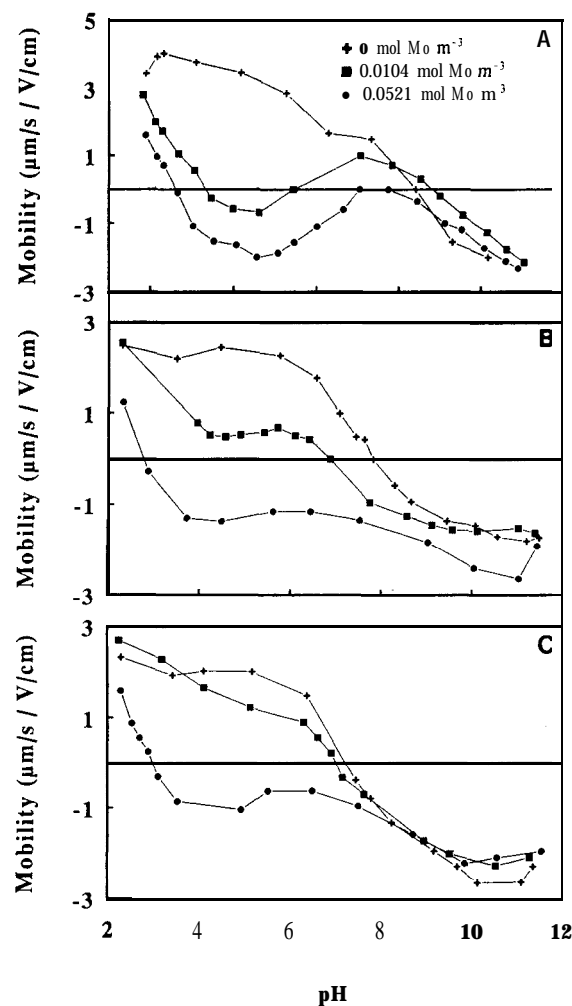


Fig. 1. Electrophoretic mobility of Fe oxides as a function of pH and total Mo concentration in NaCl solution: (a) goethite, (b) poorly crystalline goethite, (c) amorphous Fe oxide.

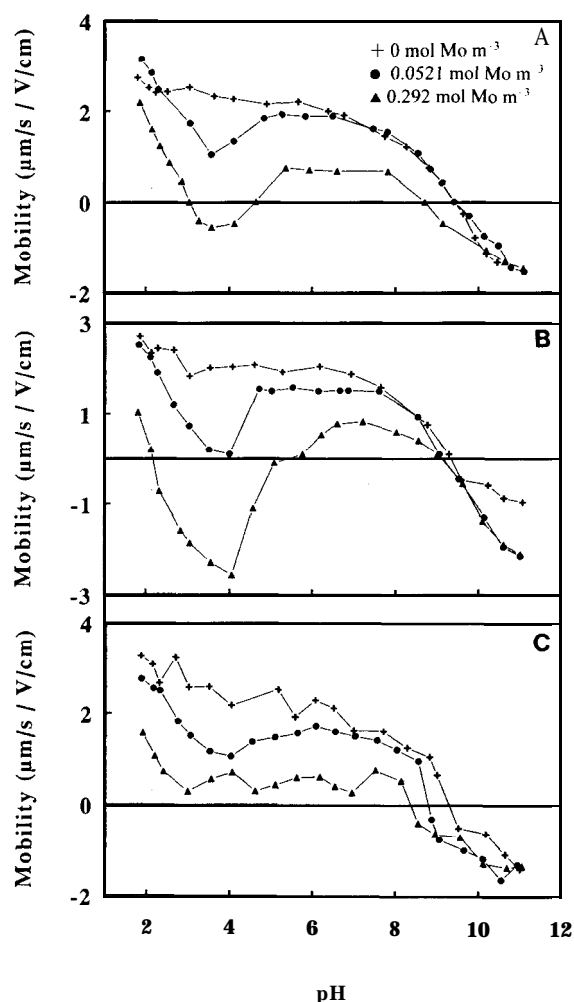


Fig. 2. Electrophoretic mobility of Al oxides as a function of pH and total Mo concentration in NaCl solution: (a) gibbsite, (b) Aluminium Oxid C, (c) amorphous Al oxide.

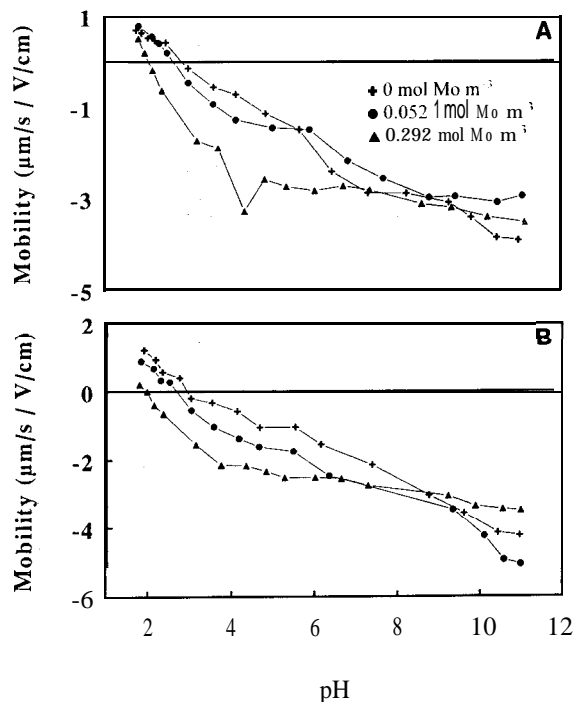


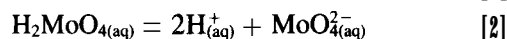
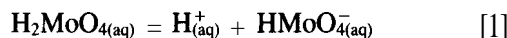
Fig. 3. Electrophoretic mobility of kaolinites as a function of pH and total Mo concentration in NaCl solution: (a) KGa-1, (b) KGa-2.

Initial Mo adsorption envelopes were carried out using $1.04 \text{ mol Mo m}^{-3}$. Subsequent experiments were carried out at $0.292 \text{ mol Mo m}^{-3}$ to avoid the formation of Mo polymers in solution (Carpeni, 1947). Baes and Mesmer (1976) suggested polymer formation above 1 mol Mo m^{-3} at pH 3 to 4 and ionic strength of 3 M . However, at ionic strength of 0.1 M ,

less polymer formation is expected. For the Al and Fe oxide minerals, initial experiments resulted in 100% adsorption throughout most of the pH range. Subsequent experiments were carried out at lower suspension density to avoid 100% adsorption and allow improved definition of the Mo adsorption envelopes.

The constant capacitance model (Stumm et al., 1980) was used to describe Mo adsorption behavior on the adsorbents. The computer program FITEQL (Herbelin and Westall, 1994) was used to fit intrinsic Mo surface complexation constants to the experimental adsorption data using the model assumptions and procedure described in detail by Goldberg and Sposito (1984a). Protonation-dissociation reactions and intrinsic conditional protonation-dissociation constants were analogous to those for the application of the constant capacitance model to B adsorption on Al and Fe oxides (Goldberg and Glaubig, 1985), clay minerals (Goldberg and Glaubig, 1986a), and soil samples (Goldberg and Glaubig, 1986b).

Molybdenum occurs as MoO_4^{2-} across most of the pH range. The acid-base reactions undergone by molybdic acid are:



the pKs, where pK is the negative logarithm of the acid dissociation constant, for these reactions are 4.00 and 8.24, respectively (Lindsay, 1979).

The surface reactions for Mo adsorption are:



where $\text{SOH}_{(\text{s})}$ represents one mole of reactive surface hydroxyls bound to a metal ion, S (Al or Fe), in the oxide or an aluminol in the clay mineral. The intrinsic conditional equilibrium con-

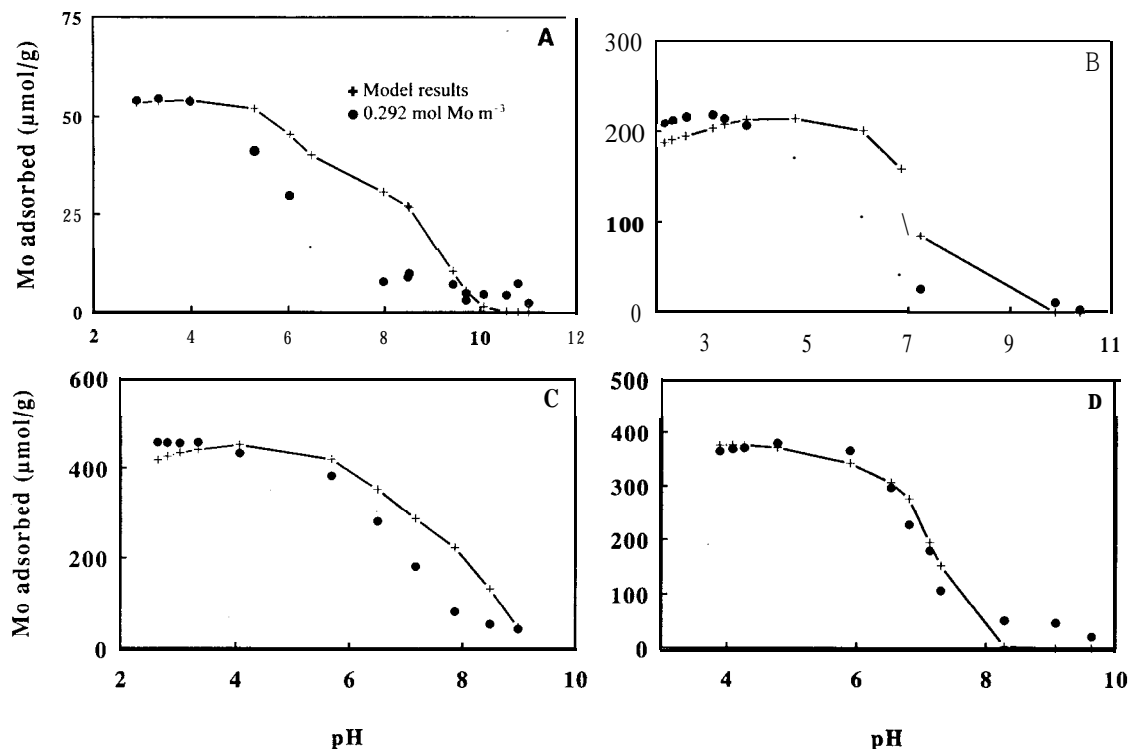


Fig. 4. Molybdenum adsorption on Fe oxides: (a) hematite, $V_\gamma = 39.6$; (b) goethite, $V_\gamma = 49.8$; (c) poorly crystalline goethite, $V_\gamma = 39.5$; (d) amorphous Fe oxide, $V_\gamma = 8.88$. Lines show model results.

stants for the Mo surface complexation reactions are:

$$K_{\text{Mo(int)}}^1 = \frac{[\text{SHMoO}_4]}{[\text{SOH}][\text{H}_2\text{MoO}_4]} \quad [5]$$

$$K_{\text{Mo(int)}}^2 = \frac{[\text{SHMoO}_4][\text{H}^+]}{[\text{SOH}][\text{H}_2\text{MoO}_4]} \exp(-F\psi/RT) \quad [6]$$

where F is the Faraday constant (C mol^{-1}), ψ is the surface potential (V), R is the molar gas constant ($\text{J mol}^{-1}\text{K}^{-1}$), T is the absolute temperature (K), and square brackets indicate concentrations (mol L^{-1}). The mass balance for the surface functional group SOH is:

$$[\text{SOH}]_{\text{T}} = [\text{SOH}] + [\text{SOH}_2^+] + [\text{SO}^-] + [\text{SHMoO}_4] + [\text{SMoO}_4^-] \quad [7]$$

The charge balance is:

$$\sigma = [\text{SOH}_2^+] - [\text{SO}^-] - [\text{SMoO}_4^-] \quad [8]$$

where σ represents the surface charge (mol L^{-1}). The surface site density was treated as MO-reactive site density and obtained from maximum Mo adsorption although we lacked evidence for 100% Mo coverage. Numerical values of the intrinsic protonation constant, $K_{\text{+}}(\text{int})$ and the intrinsic dissociation constant, $K_{\text{-}}(\text{int})$ were obtained from a literature compilation of experimental values for Al and Fe oxides (Goldberg and Sposito, 1984a). The intrinsic protonation constants were initially fixed at $\log K_{\text{+}}(\text{int}) = 7.31$, $\log K_{\text{-}}(\text{int}) = -8.80$ for goethite; $\log K_{\text{+}}(\text{int}) = 7.38$, $\log K_{\text{-}}(\text{int}) = -9.09$ for gibbsite and the clays (Goldberg and Sposito, 1984a); and $\log K_{\text{+}}(\text{int}) = 7.35$ and $\log K_{\text{-}}(\text{int}) = -8.95$ for the soils (Goldberg and Sposito, 1984b). For the clays and soils it was subsequently necessary to optimize $\log K_{\text{+}}(\text{int})$ and $\log K_{\text{-}}(\text{int})$ as well as the Mo surface complexation constants using the FITEQL program. The capacitance density was fixed at $C = 1.06 \text{ F m}^{-2}$. The constant capacitance model is often very insensitive to the value of this empirical parameter (Goldberg and Sposito, 1984a). Goodness-of-fit was indicated by the overall variance, V , in Y (Herbelin and Westall, 1994):

$$V_Y = \frac{\text{SOS}}{\text{DF}} \quad [9]$$

where SOS is the weighted sum of squares of the residuals and DF is the degrees of freedom.

RESULTS AND DISCUSSION

Points of zero charge occurred at pH 8.8 for goethite, pH 7.8 for poorly crystalline goethite, pH 7.2 for amorphous Fe oxide, pH 9.6 for gibbsite, pH 9.3 for Aluminium Oxid C and amorphous Al oxide, and pH 2.9 for kaolinites (Fig. 1-3). Previous investigations found electrophoretic mobilities of montmorillonite and soils to be negative even at pH 2 (Goldberg et al., 1993). Thus the PZCs could not be determined without dissolving these solids. For this reason electrophoretic mobilities were not determined for the 2:1 clays and soils in this study. Figures 1, 2, and 3 present the electrophoretic mobility vs. pH obtained upon adsorption of Mo onto Fe oxides, Al oxides, and kaolinites, respectively. The PZCs, considered to be the lowest pH values where a crossover occurs, are shifted to increasingly lower pH value with increasing Mo concentration. Shifting of PZC and reversal of electrophoretic mobility with increasing

ion concentration are characteristics of specific ion adsorption behavior (Hunter, 1981). The observed changes in PZC are indicative of inner-sphere surface complexation of Mo on Fe oxides, Al oxides, and kaolinites. The shape of the electrophoretic mobility curve for goethite in the presence of $0.0521 \text{ mol Mo m}^{-3}$ was virtually identical to that obtained by McKenzie (1983) for goethite in the presence of $0.104 \text{ mol Mo m}^{-3}$.

It is difficult to relate the dips in electrophoretic mobility observed in Fig. 1a, 2a, and 2b to Mo loading on the solid surface since the adsorption experiments were carried out at a higher suspension density than the electrophoretic mobility experiments. However, it appears that the crossover to positive electrophoretic mobility in the pH region 5 to 8.5 occurs where appreciable Mo adsorption is occurring. This would suggest that the mechanism of Mo adsorption on goethite, gibbsite, and Aluminium Oxid C may be changing from inner sphere to outer sphere with increasing solution pH. Simultaneous measurements of Mo adsorption and electrophoretic mobility are needed to verify this hypothesis.

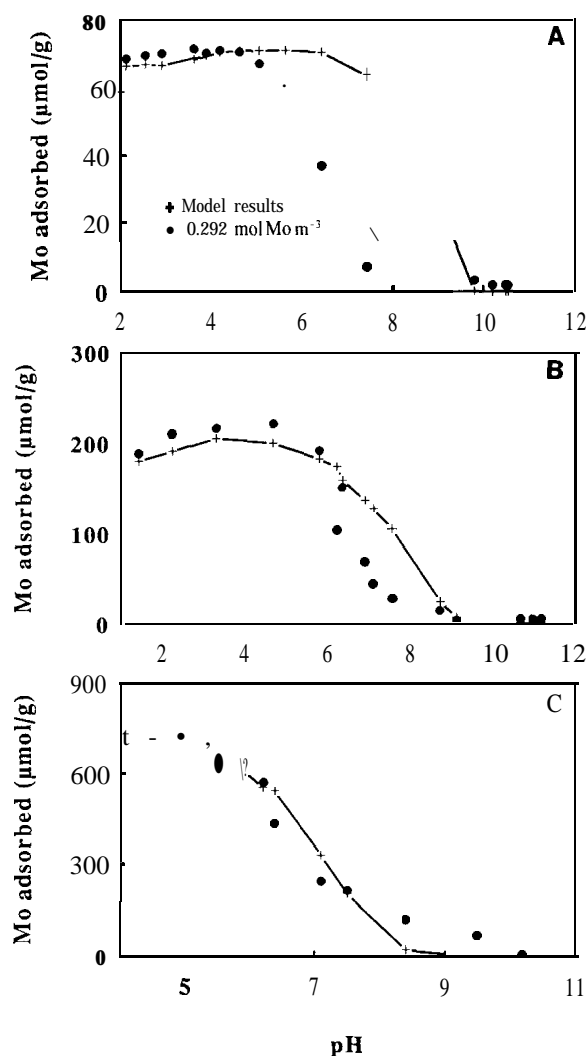


Fig. 5. Molybdenum adsorption on Al oxides: (a) Aluminium Oxid C, $V_Y = 46.6$; (b) gibbsite, $V_Y = 28.3$; (c) amorphous Al oxide, $V_Y = 4.07$. Lines show model results.

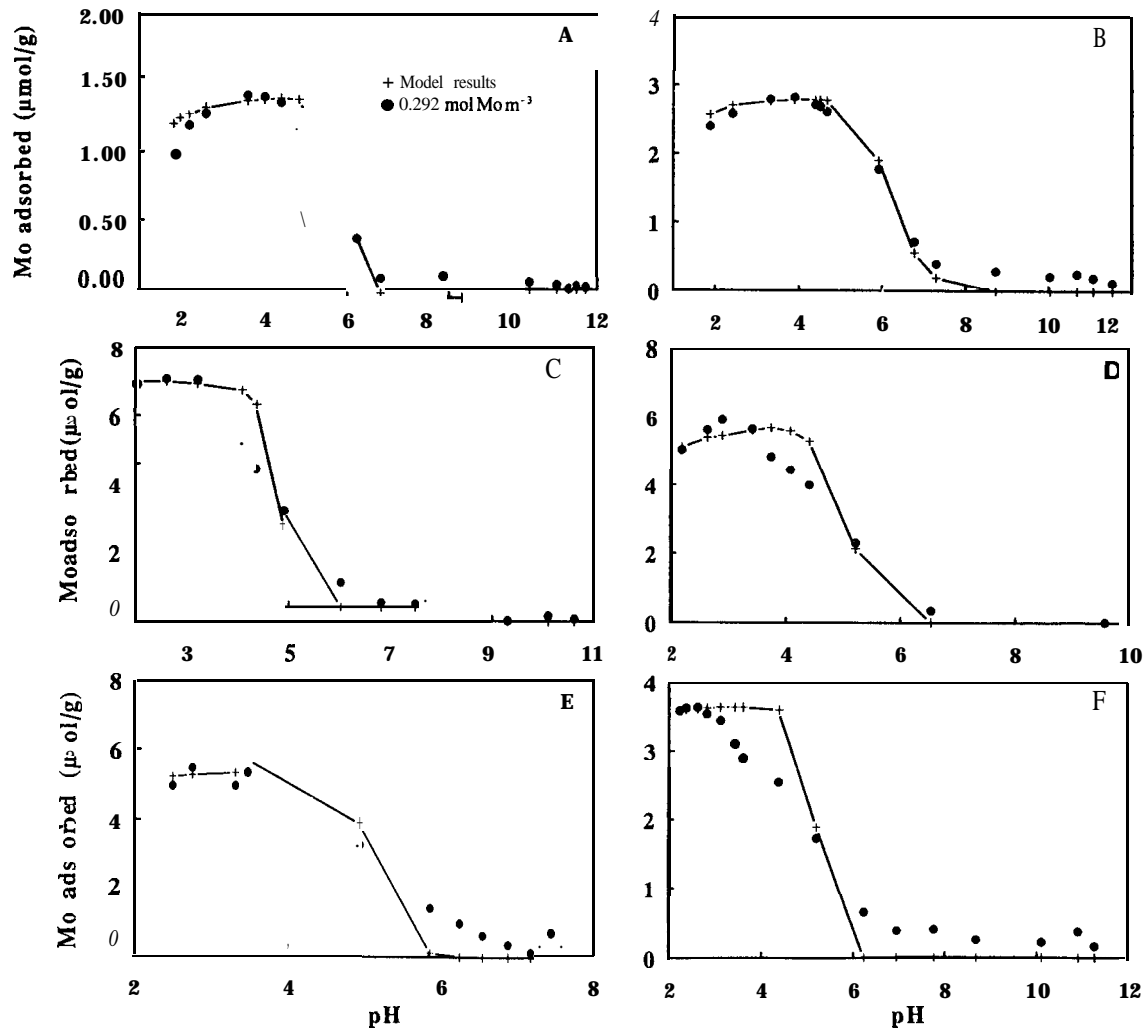


Fig. 6. Molybdenum adsorption on clay minerals: (a) KGa-1 kaolinite, $V_{\gamma} = 63.3$; (b) KGa-2 kaolinite, $V_{\gamma} = 64.1$; (c) SAz-1 montmorillonite, $V_{\gamma} = 88.8$; (d) STx-1 montmorillonite, $V_{\gamma} = 44.4$; (e) SWy-1 montmorillonite, $V_{\gamma} = 5.11$; (f) IMt-1 illite, $V_{\gamma} = 7.18$. Lines show model results.

Molybdenum adsorption as a function of pH is indicated in Fig. 4 for various Fe oxide minerals. Molybdenum adsorption exhibited a maximum at low pH that extended to about pH 4 to 5. Adsorption decreased rapidly as pH was increased from pH 5 to 8. Little adsorption occurred above pH 8. Molybdenum adsorption on a weight basis was higher for the materials having higher specific surface area and lower crystallinity. Adsorption on a weight basis increased in the order: hematite < goethite < amorphous Fe oxide < poorly crystalline goethite. A similar order of reactivity has been observed for B adsorption on Fe oxides (Goldberg and Glaubig, 1985). The shapes of our adsorption envelopes are in excellent agreement with those obtained for goethite (McKenzie, 1983; Zhang and Sparks, 1989) and hematite (Ferreiro et al., 1985). Adsorption on a per-square-meter basis increased in the order: amorphous Fe oxide < poorly crystalline goethite < goethite < hematite. It is not clear why the crystalline materials adsorbed more Mo on a per-square-meter basis.

Figure 5 shows Mo adsorption as a function of pH for various Al oxide minerals. Similar to adsorption on

Fe oxides, adsorption exhibited a maximum at low pH extending to about pH 4 to 5. Adsorption decreased rapidly from pH 5 to 8 with little adsorption occurring above pH 8. As for the Fe oxides, adsorption on a weight basis was higher for the solids having lower crystallinity. Adsorption on a weight basis increased in the order: Aluminium Oxid C < gibbsite < amorphous Al oxide. The shapes of our adsorption envelopes agree well with that obtained by Ferreiro et al. (1985) for α - Al_2O_3 . Adsorption on a per-square-meter basis increased in the order: Aluminium Oxid C < amorphous Al oxide < gibbsite. The shapes of the adsorption envelopes for Al and Fe oxides were virtually identical.

Molybdenum adsorption on clay minerals as a function of pH is depicted in Fig. 6. In contrast to the Al and Fe oxides where the adsorption maximum extends from pH 3 to 5, Mo adsorption on the clay minerals exhibits a peak near pH 3 and then decreases rapidly with increasing pH until adsorption is virtually zero near pH 7. The magnitude of Mo adsorption on a weight basis increases in the order: well-crystallized kaolinite < poorly crystallized kaolinite < illite < montmorillonite. Adsorption on

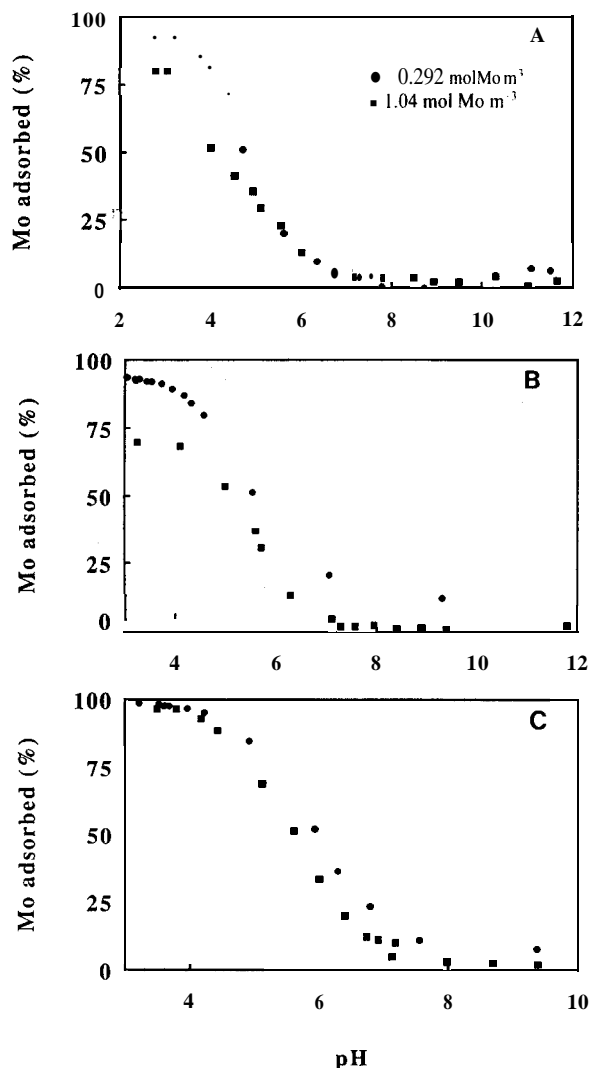


Fig. 7. Molybdenum adsorption on soils: (a) Hesperia, (b) Pachappa, (c) Porterville.

a weight basis on the clay materials is less than adsorption on all Al and Fe oxides. Similar behavior had been observed previously by Jones (1957). The shapes of our adsorption envelopes are in excellent agreement with those obtained by Jones (1957) for kaolinite and nontronite and by Theng (1971) for three soil clays dominant in kaolinite and illite. Adsorption on a weight basis increased in the order: SAz-1 montmorillonite < illite \approx KGa-2 kaolinite \approx KGa-1 kaolinite < SWy-1 montmorillonite < STx-1 montmorillonite.

Our experiments were carried out at constant total Mo concentration. It is difficult to compare adsorption per unit mass or per unit surface area when suspension density is varying between materials as in our experiments. It is possible that if the adsorption experiments had been carried out at a constant higher suspension density, the Mo adsorption on the crystalline oxides and kaolinites would have been greater.

Molybdenum adsorption as a function of pH is shown in Fig. 7 for three noncalcareous soils. Adsorption exhibited a peak near pH 3 to 4 and decreased with increasing

pH up to 7. Above pH 7 adsorption was very low. The shapes of the adsorption envelopes for the soils resembled those for the clay minerals rather than those for the Al and Fe oxides. This is logical since the Al and Fe oxide contents of the soils were low. The shapes of our adsorption envelopes are very similar to those obtained by Jones (1957) for three Australian soils. Adsorption envelopes for 0.292 and 1.04 mol Mo m⁻³ were similar in shape, indicating little effect from possible formation of Mo solution polymers. Molybdenum adsorption on the reference calcite and the two calcareous soils, Imperial and Twisselman, was low (data not shown). These results suggest that CaCO₃ is not a significant sink for Mo in soils.

The constant capacitance model was used to describe Mo adsorption on the materials studied. The model assumes an inner sphere adsorption mechanism for the Mo surface complex. The constant capacitance model was able to describe Mo adsorption on the Al and Fe oxides and the clay minerals. The model was unable to describe Mo adsorption on the soils. Table 3 provides values of the Mo surface complexation constants obtained using the FITEQL computer program (Herbelin and Westall, 1994). Molybdenum adsorption on the Al and Fe oxides was described with the model when only the Mo surface complexation constants, $K_{Mo(int)}^1$ and $K_{Mo(int)}^2$, were optimized (see Fig. 4 and 5). Optimization of the protonation-dissociation constants as well as the Mo surface complexation constants was required to describe Mo adsorption on the clay minerals (see Fig. 6). The model was unable to describe Mo adsorption on the soils since convergence of the FITEQL program either could not be obtained or provided a very bad fit. The good fit of the model to Mo adsorption on Al and Fe oxides and clay minerals suggests that inner sphere surface complexation is the appropriate adsorption mechanism for these materials. The numerical values of the Mo surface complexation constants for these materials were similar in magnitude (see Table 3), suggesting a common adsorption mechanism.

ACKNOWLEDGMENTS

Gratitude is expressed to Dr. J.D. Rhoades for providing the soil samples.

REFERENCES

- Baes, C.F., and R.E. Mesmer. 1976. The hydrolysis of cations. John Wiley & Sons, New York.
- Barrow, N.J. 1970. Comparison of the adsorption of molybdate, sulfate and phosphate by soils. *Soil Sci.* 109:282-288.
- Bibak, A., and O.K. Borggaard. 1994. Molybdenum adsorption by aluminum and iron oxides and humic acid. *Soil Sci.* 158:323-327.
- Carpeni, G. 1947. Sur la constitution des solutions aqueuses d'acide molybdique et de molybdates alcalins. IV. - Conclusions generales. *Bull. Soc. Chim. Fr.* 14:501-503.
- Cihacek, L.J., and J.M. Bremner. 1979. A simplified ethylene glycol monoethyl ether procedure for assessing soil surface area. *Soil Sci. Soc. Am. J.* 43:821-822.
- Coffin, D.E. 1963. A method for the determination of free iron oxide in soils and clays. *Can. J. Soil Sci.* 43:7-17.
- Ferreiro, E.A., A.K. Helmy, and S.G. de Bussetti. 1985. Molybdate sorption by oxides of aluminium and iron. *Z. Pflanzenernaehr. Bodenkd.* 148:559-566.

- Goldberg, S., H.S. Forster, and E.L. Heick. 1993. Boron adsorption mechanisms on oxides, clay minerals, and soils inferred from ionic strength effects. *Soil Sci. Soc. Am. J.* 57:704-708.
- Goldberg, S., and R.A. Glaubig. 1985. Boron adsorption on aluminum and iron oxide minerals. *Soil Sci. Soc. Am. J.* 49:1374-1379.
- Goldberg, S., and R.A. Glaubig. 1986a. Boron adsorption and silicon release by the clay minerals kaolinite, montmorillonite, and illite. *Soil Sci. Soc. Am. J.* 50:1442-1448.
- Goldberg, S., and R.A. Glaubig. 1986b. Boron adsorption on California soils. *Soil Sci. Soc. Am. J.* 50:1173-1176.
- Goldberg, S., and G. Sposito. 1984a. A chemical model of phosphate adsorption by soils: I. Reference oxide minerals. *Soil Sci. Soc. Am. J.* 48:772-778.
- Goldberg, S., and G. Sposito. 1984b. A chemical model of phosphate adsorption by soils: II. Noncalcareous soils. *Soil Sci. Soc. Am. J.* 48:779-783.
- Gonzalez, B.R., H. Appen, E.B. Schalscha, and F.T. Bingham. 1974. Molybdate adsorption characteristics of volcanic-ash-derived soils in Chile. *Soil Sci. Soc. Am. Proc.* 38:903-906.
- Hayes, K.F., C. Papelis, and J.O. Leckie. 1988. Modeling ionic strength effects on anion adsorption at hydrous oxide/solution interfaces. *J. Colloid Interface Sci.* 125:717-726.
- Herbelin, A.L., and J.C. Westall. 1994. FITEQL: A computer program for determination of chemical equilibrium constants from experimental data. Rep. 94-01, Version 3.1, Dep. of Chemistry, Oregon State Univ., Corvallis.
- Hunter, R.J. 1981. Zeta potential in colloid science. Principles and applications. Academic Press, London.
- Jarrell, W.M., and M.D. Dawson. 1978. Sorption and availability of molybdenum in soils of western Oregon. *Soil Sci. Soc. Am. J.* 42:412-415.
- Jones, L.H.P. 1957. The solubility of molybdenum in simplified systems and aqueous soil suspensions. *J. Soil Sci.* 8:313-327.
- Karimian, N., and F.R. Cox. 1978. Adsorption and extractability of molybdenum in relation to some chemical properties of soil. *Soil Sci. Soc. Am. J.* 42:757-761.
- Klages, M.G., and R.W. Hopper. 1982. Clay minerals in Northern Plains coal overburden as measured by x-ray diffraction. *Soil Sci. Soc. Am. J.* 45:415-419.
- Kyle, J.H., A.M. Posner, and J.P. Quirk. 1975. Kinetics of isotopic exchange of phosphate adsorbed on gibbsite. *J. Soil Sci.* 26:32-43.
- Kyriacou, D. 1967. The pH-dependence of adsorption of metallic oxyanions by ferric oxide powder. *Surf. Sci.* 8:370-372.
- Lindsay, W.L. 1979. Chemical equilibria in soils. John Wiley & Sons, New York.
- MacKenzie, R.M. 1983. The adsorption of molybdenum on oxide surfaces. *Aust. J. Soil Res.* 21:505-513.
- McLaughlin, J.R., J.C. Ryden, and J.K. Syers. 1981. Sorption of inorganic phosphate by iron and aluminium-containing components. *J. Soil Sci.* 32:365-377.
- Mikkonen, A., and J. Tummavuori. 1993. Retention of vanadium(V), molybdenum(VI) and tungsten(VI) by kaolin. *Act. Agric. Scand., Sect. B., Soil Plant Sci.* 43:11-15.
- Motta, M.M., and C.F. Miranda. 1989. Molybdate adsorption on kaolinite, montmorillonite, and illite: Constant capacitance modeling. *Soil Sci. Soc. Am. J.* 53:380-385.
- Nelson, D.W., and L.E. Sommers. 1982. Total carbon, organic carbon, and organic matter. p. 539-579. *In* A. L. Page et al. (ed.) *Methods of soil analysis, Part 2*. 2nd ed. Agron. Monogr. 9. ASA and SSSA, Madison, WI.
- Phelan, P.J., and S.V. Mattigod. 1984. Adsorption of molybdate anion (MoO_4^{2-}) by sodium-saturated kaolinite. *Clays Clay Miner.* 32:45-48.
- Reisenauer, H.M., A.A. Tabikh, and P.R. Stout. 1962. Molybdenum reactions with soils and the hydrous oxides of iron, aluminum and titanium. *Soil Sci. Soc. Am. Proc.* 26:23-27.
- Reyes, E.D., and J.J. Jurinak. 1967. A mechanism of molybdate adsorption on $\alpha\text{Fe}_2\text{O}_3$. *Soil Sci. Soc. Am. Proc.* 31:637-641.
- Roy, W.R., J.J. Hassett, and R.A. Griffin. 1986. Competitive interactions of phosphate and molybdate on arsenate adsorption. *Soil Sci.* 142:203-210.
- Roy, W.R., J.J. Hassett, and R.A. Griffin. 1989. Quasi-thermodynamic basis of competitive-adsorption coefficients for anionic mixtures in soils. *J. Soil Sci.* 40:9-15.
- Sims, J.T., and F.T. Bingham. 1968. Retention of boron by layer silicates, sesquioxides, and soil materials: II. Sesquioxides. *Soil Sci. Soc. Am. Proc.* 32:364-369.
- Spanos, N., L. Vardonis, Ch. Kordulis, and A. Lycourghiotis. 1990a. Molybdenum-oxo species deposited on alumina by adsorption. I. Mechanism of the adsorption. *J. Catal.* 124:301-314.
- Spanos, N., L. Vardonis, Ch. Kordulis, P.G. Koutsoukos, and A. Lycourghiotis. 1990b. Molybdenum-oxo species deposited on alumina by adsorption. II. Regulation of the surface Mo^{VI} concentration by control of the protonated surface hydroxyls. *J. Catal.* 124:315-323.
- Sposito, G. 1984. The surface chemistry of soils. Oxford Univ. Press, New York.
- Stumm, W., R. Kummert, and L. Sigg. 1980. A ligand exchange model for the adsorption of inorganic and organic ligands at hydrous oxide interfaces. *Croat. Chem. Acta* 53:291-312.
- Theng, B.K.G. 1971. Adsorption of molybdate by some crystalline and amorphous soil clays. *N. Z. J. Sci.* 14:1040-1056.
- Vardonis, L., P.G. Koutsoukos, and A. Lycourghiotis. 1990. Adsorption of molybdates on doped γ -aluminas in alkaline solutions. *Colloids Surf.* 50:353-361.
- Xie, R.J., and A.F. MacKenzie. 1991. Molybdate sorption-desorption in soils treated with phosphate. *Geoderma* 48:321-333.
- Xie, R.J., A.F. MacKenzie, and Z.J. Lou. 1993. Causal modeling pH and phosphate effects on molybdate sorption in three temperate soils. *Soil Sci.* 155:385-397.
- Zhang, P.C., and D.L. Sparks. 1989. Kinetics and mechanisms of molybdate adsorption/desorption at the goethite/water interface using pressure-jump relaxation. *Soil Sci. Soc. Am. J.* 53:1028-1034.